Available online at http://www.journalcra.com

International Journal of Current Research
Vol. 3, Issue, 11, pp.405-412, October, 2011

INTERNATIONAL JOURNAL OF CURRENT RESEARCH

ISSN: 0975-833X

RESEARCH ARTICLE

AN ASYMPTOTIC SOLUTION OF ROTATING BIO-CONVECTION (RCB) IN A SUSPENSION OF PHOTOTACTIC ALGAE

***[1]Prof. Dr. P.K. Srimani and [2]Sujatha, D.**

[1]Former Chairman, Department of Computer Science and Mathematics, Bangalore University, Director, R&D, B.U, Bangalore.
[2]H.O.D. Department of Mathematics, B.M.S. College for Women, Bangalore

ARTICLE INFO

Article History:
Received 7th June, 2011
Received in revised form
5th August, 2011
Accepted 9th September, 2011
Published online 30th October, 2011

Key words:
Rotating
Bioconvection,
Microorganisms,
Stability, Asymptotic analysis,
Phototaxis, solvability conditions.

ABSTRACT

This paper deals with the asymptotic analysis of Rotation Bio convection (RBC) in a suspension of phototactic algae. Bioconvection is an interesting pattern-forming phenomenon driven by the swimming activity of various aquatic micro organisms. In fact, bioconvection is a robust phenomenon and is one of the oldest documented collective behavior of independent microorganisms. Further, positive phototaxis consists of motions directed toward the source of illumination and negative phototaxis is, the motion directed away from it. The asymptotic analysis was carried up to the fourth order approximation and the cumulative effect of Taylor number and the other governing parameters on the stability conditions as well as on the different profiles was remarkable. The computed results were presented through graphs and are in excellent agreement with the available results in the limiting case.

INTRODUCTION

Bio-convention is an intriguing pattern forming phenomenon driven by swimming activity of various aquatic micro-organisms. The term Bio-convention was recently developed in fluid mechanics and refers to flows induced by the collective motion of a large number of motile micro-organisms (platt, 1961, Pedley and Kessler 1992). This phenomenon can lead to pattern formation in aquous media when the motile micro organisms respond to certain stimuli (e.g. Gravity , Light, Nutrients etc.).This tactic nature of the microorganisms leads to different types of bio-convection (B.C). In general, Bio-convection has a positive effect on the entire microbial population by carrying oxygen into deep layers of non-aerated suspensions. Further positive phototaxis consists of motions directed towards the source of illumination and negative photo taxis is, the motion directed away from it. The basic mechanism underlying this phenomenon is similar to that of the well known R.B.Convention in the sense that both are due to the Buoyancy force resulting from a density gradient, which in the case of BC, occurs when a large number of micro organisms (that are slightly denser than water) accumulates in a certain region of the fluid medium, while in the case of R.B.Convection, the density gradient is due to the adverse temperature gradient. Applications of bio convection to enhance mixing of small solid particles may include micro fluidic applications relevant to bio-technology and medicine, such as the analysis of blood samples when only limited volumes of blood can be extracted. These are other interesting applications. A detailed review of the literature is available in Padmasani (2003) Anuradha (2006) and Hill and Pedley (2005). In the present model the constraining effect of rotation along with the effect of shading whereby micro organisms nearer the light source absorb and scatter the light before it reaches those farther away. The present model constitutes five dimensionless parameters together with a parameter that specifies the vertical position of the sub layer in the fluid. Our model considers two cases (i) Rigid upper surfaces (ii) Stress free upper surface. The asymptotic analysis was carried up to the fourth order approximation. The cumulative effect of Taylor number and the other governing parameters on the stability conditions as well as on the different profiles is remarkable. The position of the sub layer actually depends on the intensity of the light source and the solution are obtained through the solvability conditions. The computed results are presented through graph and are in excellent agreement with the available results in the limiting cases.

Corresponding author: sujathabms@yahoo.com

MATERIALS AND METHODS

In this section the continuum model in boundary conditions and asymptotic analysis are discussed.

THE CONTINUUM MODEL:

In this study it is assumed that the length scale of the bulk motions and the concentration distribution are large compared to typical cell diameters and cell spacing.

The algal cells themselves are modeled as internally homogeneous, pigmented particles of volume v and density $\rho + \Delta\rho (\Delta\rho << \rho,$ where p is the density of the fluid) and posses the same light transmittance in all orientations. The number of cells in a small volume δ v defined relative to Cartesian axis O x* y* z* in n*(x*,t*) δ v Where z* is the axis in the vertical direction and t* is time. Neglecting all inertia in the cells motion and supposing the suspension is dilute (n* v << 1) and incompressible then, if u*(x*,t*) is average velocity of all the material in δ v,

$$\nabla^* \cdot U^* = 0 \qquad \ldots(1)$$

For simplicity, we shall assume that the effect of the cells, on the suspension is dominated by the stokelets due to their negative buoyancy and that all other contributions to the bulk stress are sufficiently small to be neglected. Neglecting all the forces on the fluid except the cells negative buoyancy, n*vg $\Delta\rho$ δv where g is the acceleration due to gravity, the momentum equation under the boussinesq approximation is

$$\rho\left[\frac{Du^*}{Dt^*} + 2\vec{\Omega}\hat{k} \times u^*\right] = -\nabla^* P_e^* - n^* vg\hat{k} + \mu\nabla^{*2} u^* \qquad \ldots(2)$$

The entire system is rotating about the vertical axis with an angular velocity $\vec{\Omega}$ =(0,0, Ω). Here, $\frac{D}{Dt^*} = \frac{\partial}{\partial t^*} + u^*, \quad \nabla^*$ is the material time derivative. $\hat{k}$ is a unit vector in the z* direction, P_e is the excess pressure above hydrostatic and μ is the dynamic viscosity of the suspension which, since the suspension is dilute, is considered to be that of the fluid, which is effectively water, The equation for cell conservation is

$$\frac{\partial n^*}{\partial t^*} = -\nabla^*, J^* \qquad ..(3)$$

where J* (x*, t*) δ s is the net flux across a surface element, δ s, at x*, j* can be written as

$$J^* = n^* u^* + n^* v_e \overline{p} - D^* \nabla^* n^* \qquad \ldots(4)$$

where $\overline{p}$ is given by $V_c = V_A \overline{p} = V_A \int \hat{p} f(\hat{p}) d\hat{p}$

The first term, n*. u*, is the flux due to advection of cells by the bulk flow. The other terms represent fluxes arising from the stochastic nature of the cell swimming: n* $v_c \overline{p}$ is a mean flux due to cell swimming and –D*, ∇^* n* is a diffusive flux of cells down cell concentration gradients. We shall consider a fluid layer with horizontal boundaries at z* = -H, O and shall assume that the vertical boundaries are far enough away that the layer has an effectively infinite width. The suspension is illuminated by parallel light from a uniform source of intensity I_s Vertically above the layer.

$$\overline{P} = \Lambda I_c \alpha^* \left(\int_{z^*}^{o} n^*(x^1, t^*) dz^1 - CHN_0\right)\hat{k} \qquad ..(5)$$

The continuum model is now complete.

THE BASIC STATE

This study presents the results for both free and rigid upper horizontal boundaries. The basic state solution is found to be;

$$n^*(z^*) = \frac{k^{*2} D_v}{2V_A \Lambda I_c \alpha^*} Sech^2\left(\frac{1}{2} k^*(z^* + CH)\right) \qquad ..(6)$$

where k* is a constant of integration which can be related to N_0 the number of cells per unit volume for the whole layer, by the relation $\int_{-n}^{0} n^*(x^1) dz^1 = N_0 H$ ..(7)

It is apparent from (6) that the region above z* = -CH is locally gravitationally stable and convective motions occurring in the unstable region below z*= -CH will penetrate the upper layer.

Non-Dimensionalization

The governing equations are made dimensionless using the following scales: Length Scale: H(H is depth of the layer), Bulk fluid velocity: Dv/H; Time: H^2 / Dv; Cell Concentration : N_0 , N_o is the uniform cell concentration , Diffusion:Dv, Pressure: $vD_v\rho / H^2$ v is the kinematic viscosity and D_v is the diffusion parameter.

$$U = 0,$$

$$n(z) = \frac{K^2}{2d} Sech^2\left(\frac{1}{2} K(z + c)\right) \qquad \}\ldots(8)$$

where the horizontal boundaries are at z = -1, 0

and $d = \frac{HV_A P}{D_v}$ *where* $P = \Lambda I_c \alpha^* N_o H$ … (9)

K=k·H and is determined by (7) which produces the transcendental equation

$$K\left(\tanh(\frac{1}{2}kc) - \tanh(\frac{1}{2}k(c-1))\right) = d \qquad \ldots(10)$$

After non dimensionalizing, the system of equations becomes

$$\nabla \cdot U = O$$

$$\frac{\partial n}{\partial t} = -(\nabla n.U) - d\frac{\partial n}{\partial z}\left[\int n(x^1) dz - c\right] - dn\frac{\partial}{\partial z}\left[\int n(x^1) dz - c\right] + K\nabla_h^2 n + \frac{\partial^2 n}{\partial z^2} \qquad ..(11)$$

$$Sc^{-1}\left[\frac{\partial U}{\partial t} + (U.\nabla)U\right] + \frac{2H^2}{v}\left[\Omega\hat{k}xU\right] = -\nabla Pc - \beta n\hat{k} + \nabla^2 U) \ldots(12)$$

Linear Stability analysis

In this section, the linear stability problem is discussed by considering a small perturbation to the equilibrium state (8) of amplitude $\in$, Where $0 < \in \leq 1$ In this case.

$$U = \in U_1, \quad n = n_0 + \in n_1(x,t), \quad P_c = P_o + \in P_e$$

where $n_0 = \frac{K^2}{2d} Sech^2\left(\frac{1}{2} K(z + c)\right)$ ...(13)

If $u_1 = (u_1, v_1, w_1)$ and we define $D_H = \kappa D_v$ Where K is a positive real number then, substituting the above perturbation quantities into (1) (2) and (3) and linearizing about the basic state by collecting the 0($\in$) terms, gives.

$$\nabla U_1 = 0 \qquad ...(14)$$

$$Sc^{-1}\frac{\partial U_1}{\partial t}+\frac{2H^2}{v}\left(\Omega\hat{k}XU_1\right)=-\nabla pe-\beta n_1(x,t)\hat{k}+\nabla^2U_1 \quad ...(15)$$

$$\frac{\partial n_1}{\partial t}+d\left[\frac{dn_0}{dz}\int_z^0 n_1(x,y,s,t)ds+(\int_z^0 n_0(s)ds-c)\frac{dn_1}{dz}-2n_0n_1\right]-\kappa\nabla_n^2n_1-\frac{\partial^2n_1}{\partial z^2}=-w_1\frac{dn_0}{dz} \quad ...(16)$$

where $\beta=\frac{N_0V\Delta\rho gH^3}{\rho D_v\nu}$ where $S_c=\frac{v}{D_v}$ is the schimid number, $\nabla_h^2=\frac{\partial^2}{\partial x^2}+\frac{\partial^2}{\partial y^2}$, p_e and the horizontal Component of u is have eliminated from the above equations by taking the curl of (15) twice and retaining the z-component of the result. This reduces the system to two equations in w_1 and

$$n_1\left[Sc^{-1}\frac{\partial}{\partial t}-\nabla^2\right]^2\nabla^2w_1+\Gamma^2\frac{\partial^2w_1}{\partial z^2}=-\left[Sc^{-1}\frac{\partial}{\partial t}-\nabla^2\right]\beta\nabla_h^2n_1 \quad (17)$$

$$\frac{\partial n_1}{\partial t}+d\left[\frac{dn_0}{dz}\int_z^0 n_1(x,y,s,t)ds+(\int_z^0 n_0(s)ds-c)\frac{dn_1}{dz}-2n_0n_1\right] \quad ...(18)$$

$$-k\nabla_n^2n_1-\frac{\partial^2n_1}{\partial z^2}=-w_1\frac{dn_0}{dz}$$

where $\frac{2H^2\Omega}{v}=\Gamma$ (Γ is Taylor number) ...(19)

The equations in w_1 and n_1 can then be resolved into normal modes by substitutions

$$n_1=\phi(z)f(x,y)\exp(\sigma t),\quad w_1=w(z)f(x,y)\exp(\sigma t) \quad ...(20)$$

Where the horizontal platform satisfies $\nabla_h^2f=-k^2f$, k being a dimensionless horizontal wave number and σ is the growth rate. Using (33) the governing equations after the elimination of pressure and vertically becomes

$$\left(\sigma Sc^{-1}+k^2-\frac{d^2}{dz^2}\right)^2\left(k^2-\frac{d^2}{dz^2}\right)w-\Gamma^2\frac{d^2w}{dz^2}= \quad ...(21)$$

$$-\beta k^2\phi\left(\sigma Sc^{-1}+k^2-\frac{d^2}{dz^2}\right)k^2\phi$$

$$d\frac{dn_0}{dz}\int_z^0\phi(s)ds+\left\{\begin{array}{l}\left(\sigma-2dn_0+\kappa k^2\right)+\\ d\left(\int_z^0 n_0(s)ds-c\right)\frac{d}{dz}-\frac{d^2}{dz^2}\end{array}\right\}\phi=-\frac{dn_0}{dz}w \quad ....(22)$$

Subject to boundary conditions

$$\frac{d\phi}{dz}-d\left\{\left(\int_z^o n_0(s)ds-c\right)\phi+n_0\int_z^0\phi(s)ds=0\right. \quad \text{at z=-1,0} \quad ...(23)$$

and for rigid boundaries

$$w=\frac{dw}{dz}=\frac{d^3w}{dz^3}=0 \quad \text{at z = -1,0} \quad ..(24)$$

At a stress free surface the last condition Is replaced by

$$w=\frac{d^2w}{dz^2}=\frac{d^4w}{dz^4}=0 \quad \text{at z = -1,0} \quad ...(25)$$

The new aspect of this model, the effects of photo-tactic motions, are incorporated in the terms found on the left hand side of the cell flux Equation.

$$\left(\frac{dn_0}{dz}\right)\int_z^0\phi ds,\ n_0\phi \ \text{and}\ \left(\int_z^0 n_0(s)ds-c\right)\frac{d\phi}{dz}$$

Equation (22) is a linear integro differential equation with non constant co-efficient, solution of which represents a problem of considerable difficulty. Certainly it may be reduced to ODE by the use of the substitution.

$$\phi^*(z)=\int_z^0\phi(s)ds \quad ...(26)$$

In which case $\phi^{*1}(z)=-\phi(z)$

Asymtotic Solutions

In this section we shall present an asymptotic solution to the normal mode problem for rigid and stress free upper surfaces when 0 < d << 1. In the case when d << 1, (24) can be solved approximately to give $k\approx(2d)^{1/2}$ so that n(z) is given by (21). Motivated by the studies of CLS and HPK, we anticipate that for this shallow layer case the most unstable wavelength is zero when C=0. Thus we consider small wave numbers such that $k\ll d$ and we get,

$$\left(\sigma Sc^{-1}+\tilde{k}^2d^2-\frac{d^2}{dz^2}\right)^2\left(\tilde{k}^2d^2-\frac{d^2}{dz^2}\right)w-\Gamma^2\frac{\partial^2w}{\partial z^2}=R\tilde{k}^2d\frac{d\phi^*}{dz}$$

$$\left(\sigma Sc^{-1}+\tilde{k}^2d^2-\frac{d^2}{dz^2}\right) \quad ...(27)$$

$$d\frac{dn_0}{dz}\phi^*(z)-\left[\sigma-2dn_0+\kappa\tilde{k}^2d^2\right]$$

$$\frac{d\phi^2}{dz}-d\left(\int_z^o n_0(s)ds-c\right)\frac{d^2\phi^*}{dz^2}+\frac{d^3\phi^*}{dz^3}=-\frac{dn_0}{dz}w \quad ...(28)$$

$$R=\beta d=\frac{N_0V\Delta\rho gH^3d}{\rho D_v\nu} \quad ...(29)$$

here $\tilde{k}=k/d$ so $\tilde{k}\ll 1$. On expanding the hyperbolic functions as power series in d we get

$$n_0=1+ds_1(z)+d^2s_2(z)+0(d^3)$$

$$\frac{dn_0}{dz}=d\frac{ds_1}{dz}+d^2\frac{ds_2}{dz}+0(d^3)$$

$$\int_z^0 n_0(z^1)dz^1-C=$$

$$-(z+c)+d\int_z^0 s_1(z^1)dz^1+d^2\int_z^0 s_2(z^1)dz^1+0(d^3)$$

where $s_1(z)=-\frac{1}{2}(z^2+2zc+c-\frac{z^1}{3})$

$$s_2(z)=-\frac{1}{6}(z^4+4z^3c+3z^2c^2-2zc^3+3z^2c+6zc^2-c^3-z^2-2zc+2c^2-c+\frac{2}{15})$$

HPK observed that to get nontrivial solution which satisfy the even leading order boundary conditions, requires that highest derivations in (45) and (46) are retained and the leading order balance in (45) must give.

$$\left(\frac{d^2}{dz^2}-\sigma s_c^1\right)\frac{d^2w}{dz^2}=d\tilde{k}^2R\frac{d\phi}{dz} \quad . \qquad \ldots(30)$$

(30) represents the balance between the viscous terms on the left hand side and the buoyancy terms on the right hand side which drive without loss of generality, we specify that

$$\phi^* = 0(1) \qquad \ldots(31)$$

To be consistent with (47) and (50) we consider the case $\phi^* \square 1, w \square d, R \square 1, \sigma \square 1$ and expand the following quantities as power series in d:

$$\phi^*=\sum_{n=0}^{\infty}d^n\phi_n^*,\ w=\sum_{n=1}^{\infty}d^nw_n,\ \ R=\sum_{n=0}^{\infty}d^nR_n,\ \ \sigma=\sum_{n=0}^{\infty}d^n\sigma_n$$

Case (i) : **Rigid upper surface**

Leading order problem

$$\frac{d^6w_1}{dz^6}+2Sc^{-1}\sigma_0\frac{d^4w_1}{dz^4}-Sc^{-2}\sigma_0^2\frac{d^2w_1}{dz^2}+\Gamma^2\frac{d^2w^1}{dz^2}=$$

$$\tilde{k}^2Sc^{-1}R_0\sigma_0\frac{d\phi_0^*}{dz}-\tilde{k}^2R_0\frac{d^3\phi_0^*}{dz^3} \qquad \ldots(32)$$

$$\frac{d^3\phi_0^*}{dz^3}-\sigma_0\frac{d\phi_0^*}{dz}=0 \qquad \ldots(33)$$

subject to the boundary conditions

$$\frac{d^2\phi_0^*}{dz^2}=w_1=\frac{dw_1}{dz}=\frac{d^3w_1}{dz^3}=0 \quad \text{at } z=-1,0. \qquad \ldots(34)$$

$$\phi_0^*=0 \quad \text{at } z=0 \qquad \ldots(35)$$

Integrating (50) w.r.t z and applying Boundary conditions we get

$$\Rightarrow \quad \sigma_0=0 \quad \text{Or} \quad \phi_0^*(-1)=0$$

We now have the following two cases:

When $\phi_0^*(-1)=0 \quad \sigma_0\neq 0$

$\sigma_0<0 \qquad \phi_0^*(z)=Sinn\pi z$

$\sigma_0>0 \Rightarrow \phi_0^*(z)$ *has trivial solution*

when $\sigma_0=0$ then

$$\frac{d^2\phi_0^*(2)}{dz^2}=0 \ \Rightarrow \phi_0^*(z) = -z \qquad \ldots(36)$$

Suppose $\sigma_0=0$

$$\frac{d^6w_1}{dz^6}+\Gamma^2\frac{d^2w_1}{dz^2}=\tilde{k}^2R_0\frac{d^3\phi_0^*}{dz^3}$$

Solving the above equation and applying the boundary conditions we get

$$w_1=\tilde{k}^2R_0\left\{\left(\frac{\Gamma^2}{8!}\right)z^8-\left(\frac{1}{4!}\right)z^4-\left(\frac{\alpha}{3!}\right)z^3-\left(\frac{\beta}{2}\right)z^2\right\} \qquad \ldots(37)$$

$$\alpha=\frac{1}{2}-\frac{9}{2.7!}\Gamma^2 \quad \beta=\frac{1}{12}-\frac{5}{4.7!}\Gamma^2$$

Which is precisely the same as leading order solution as that obtained by HPK where ϕ_0^* has been scaled so that $\phi_0^* = +1$ without loss of generality. Proceeding in the same manner, we compute the highest order solutions which are listed below (the details are avoided);

Solution

$$\sigma_1=0$$

$$\phi_1^*=\frac{1}{3}z^3+\frac{1}{2}cz^2 \qquad \ldots(38)$$

$$w_2=-\tilde{k}^2R_0\left(\frac{2\Gamma^2}{10!}z^{10}+\frac{c\Gamma^2}{9!}z^9-\frac{2}{6!}z^6-\frac{c}{5!}z^5\right)_1$$

$$-\tilde{k}R_1\left\{\frac{\Gamma^2}{8!}z^8+\frac{1}{4!}z^4\right\}+\frac{K1}{3!}z^3+\frac{k_2}{2}z^2 \qquad \ldots(39)$$

$$k_1=\tilde{k}R_0\left[\frac{1}{5}\left(\frac{1}{3}-\frac{3c}{4}\right)-\frac{\Gamma^26}{9!}\left(\frac{8}{5}-7c\right)\right]\ \tilde{k}R_1\frac{1}{2}\left(1-\frac{9}{7!}\Gamma^2\right)$$

$$k_2=\tilde{k}R_0\left[\frac{1}{30}\left(\frac{1}{3}-c\right)-\frac{\Gamma^2}{3.8!}\left(\frac{14}{15}-4c\right)\right]-\frac{\tilde{k}R_1}{4}\left[\frac{1}{3}-\frac{5\Gamma^2}{7!}\right]$$

$$\sigma_2=\tilde{k}^2R_0\left\{\frac{-\Gamma^2}{10!}(9-10c)+\frac{1}{6!}(5-6c)-\frac{\alpha}{5!}(4-5c)+\frac{\beta}{4!}(3-4c)\right\}-\tilde{kk}^2 \qquad \ldots(40)$$

$$\phi_2^*=\tilde{k}^2R_0\left\{\frac{-9\Gamma^2}{12!}z^{12}-\frac{d\Gamma^2}{11!}z^{11}+\frac{5}{8!}z^8+\frac{1}{7!}(4\alpha+c)z^7+\frac{1}{6!}(3\beta+\alpha c)z^6\right\}$$

$$-\frac{1}{5!}\left\{\tilde{k}R_0\beta c+12\right\}z^5-\frac{c}{3}z^4-\frac{1}{6}\left\{\left(c^2+c-\frac{1}{3}\right)+k_3\right\}z^3+z \qquad \ldots(41)$$

$$k_3=\tilde{k}^2R_0\left\{\frac{-\Gamma^2}{10!}(9-10c)+\frac{1}{6!}(5-6c)-\frac{\alpha}{5!}(4-5c)+\frac{\beta}{4!}(3-4c)\right\}$$

$$R_0=\frac{k}{\frac{-\Gamma^2}{10!}(9-10c)+\frac{1}{6!}(5-6c)-\frac{\alpha}{5!}(4-5c)+\frac{\beta}{4!}(3-4c)} \qquad \ldots(42)$$

$$\sigma_3=\frac{\tilde{kR}_0}{6!}\left\{\begin{array}{l}\frac{1}{420}\left(280C^3-420C^2+223C-43\right)+\\ \frac{\Gamma^2}{504}\left(-\frac{5}{3}C^3+\frac{9}{5}C^2-\frac{533}{1320}C-\frac{97}{2100}\right)\end{array}\right\}$$

$$-\tilde{k}^2R_1\left\{\frac{1}{6!}\left(c-\frac{1}{2}\right)+\frac{\Gamma^2}{8!}\left(\frac{3}{20}-\frac{5c}{18}\right)\right\} \qquad \ldots(43)$$

$$R_1=-\frac{\left\{\frac{1}{420}\left(280C^3-420C^2+223C-43\right)-\frac{\Gamma^2}{504}\left(\frac{5}{3}C^3-\frac{9}{5}C^2+\frac{533}{1320}C+\frac{97}{2100}\right)\right\}}{\left(C-\frac{1}{2}\right)+\frac{\Gamma^2}{56}\left(\frac{3}{20}-\frac{5c}{18}\right)} \qquad \ldots(44)$$

CASE(ii): STRESS FREE SURFACE

$$w_1 = -\tilde{k}^2 R_0 \left\{ \frac{z^4}{4!} - \Gamma^2 \frac{z^8}{8!} + \alpha_1 \frac{z^3}{3!} + \beta_1 z \right\} \quad \ldots(45)$$

$$\alpha_1 = \frac{9}{4!} - \Gamma^2 \frac{21}{8!}, \qquad \beta_1 = \frac{-1}{2.4!} + \frac{5}{2}\frac{\Gamma^2}{8!}$$

$$\sigma_2 = \tilde{k}^2 R_0 \left\{ \frac{1}{6!}(5-6c) - \frac{\Gamma^2}{10!}(9-10c) - \frac{\alpha_1}{5!}(4-5c) - \frac{\beta_1}{3!}(2-3c) \right\} - k\tilde{k}^2 \quad (59)$$

RESULTS AND DISCUSSIONS

The results of the present investigation are presented in figures 1 to 18. The results are computed for different sets of the governing parameters (k,d,c,t) for rigid upper and stress free upper surfaces. The results for small as well as large rotation rates are presented through graphs. The following important observations were made from the figures: In figures 1 to 6, the velocity profiles are drawn for different combinations of the governing parameters. W(z) is negative throughout the region only when d=20 and c=0.8 as in the non-rotating case where c=0.2. For d < 20 ,the profile is parabolic with maximum a value at the middle of the layer. The parabolic nature strongly depends on the values of d and C in the rotating bioconvective case. The effect of increasing c is to decrease w (z) for a particular wavenumber k. For small as well as large values of d ,w=o as k → 0, irrespective of the values of t and c, which is as expected (figures 5 and 6).For all non-vanishing values of k, w increases continuously with k for a particular value of c both in the shallow as well as deep layers. Further, for large rotation rate (t=10^3), the vertical velocity W is very high in the case of a shallow layer when compared to a deep layer (figures 5a and 5b).It is interesting to note(figures 5c and 6a) that the effect of rotation in BPC is quite remarkable, for w decreases with the increase in c for t=1000 but , for t=10, w increases with c for a particular k. (Ii) In figures 7 and 8, the variation of total R with respect to c is presented for t=100, d=10; t=10 and d=0.1 respectively. The interesting feature is that for d=10 and t=100, as c is increased R(k) vs. c curve exhibits oscillations. In other words, the branching is mode 2 and not mode 1, in which case, a single convection cell that extends throughout the whole layer is supplemented by a second smaller convection cell which forms at the bottom of the layer and grows in the height for c ≤ 0.75.For values of c< 0.7, it is mode 1. Thus mode 2 solutions were observed in this analytical investigation for certain restricted parametric ranges.

From figures 9 and 10, it is observed that as d is increased for t=1000,the value of R increases. Further, it is found that the value of c for which the suspension is most unstable increases as d increases for a certain ranges of the Taylor number. This type of behavior is observed in the case of penetrative convection see for example, veroniss (1963),Whitehead and Chen(1970), Rudraiah and srimani (1980), Srimani (1981), Srimani and Sudhakar (1992) and Mathews(1988). Veronis (1963) and Srimani and Sudhakar (1994) have reported that the introduction of a locally gravitationally stable region of fluid or a porous layer under the rotational constraint above an unstable region decreased the critical Rayleigh number and suggested that the addition of a stable fluid at the top of the layer was offset by the relaxation of the upper no-slip boundary conditions and thus allowing greater penetration into the stable region, so that the fluid motion could achieve an optimum level. In the present investigation, as the values of c and t are increased in a suitable fashion, the relaxation of the no-slip boundary conditions and the introduction of the rotational constraint which reduces the viscous dissipation, are offset by the addition of stable fluid at the top of the layer. Where the buoyancy tends inhibit the convective fluid motions thereby increasing R again.

Figures 9 and 10 predict the linear behavior of R in shallow as well as deep layers for t=1000 and different values of c. In figures 11 and 14, the profiles of perturbations to the shading Q (z) for deep and shallow layers are presented for different values of c and t. The following observations are made: For large rotation rates, the profiles exhibit the same behavior for shallow as well as deep layers. The values were almost identical and decreases with c. For values of c ≤ 0.7, Q decreases enormously with k and vanishes for k=1. But for small rotation rates, for example, t=10, the behavior is exactly the opposite. In this case Q (z) increases with c and k and the shading never becomes zero. This clearly suggests that there is a drastic change in the behavior of rotating and non-rotating bioconvective systems in the presence of phototaxis. (iv) In figures 15 to 18, the vertical velocity profiles for shallow as well as deep layers are presented when the upper boundary is a stress-free surface. Figures 15 and 16, reveal that there is a drastic difference in the behavior of w for small and large rotation rates when d=0.1.In the case of deep layer, large rotation rate (t > 10^2) has no additional effect on w. Finally it is concluded that there is a remarkable difference in the behavior of a bioconvective system (with phototaxis) with regard to (a) rotating and non-rotating system and (b) shallow and deep layers. Since the effect of rotation is quite significant it is possible to suppress or enhance bioconvection by a suitable choice of the governing parameters. Further, it is emphasized that the result of the present investigation are in excellent agreement with those of non-rotating system (Vincent & Hill, 1996) for t=o for all the cases.

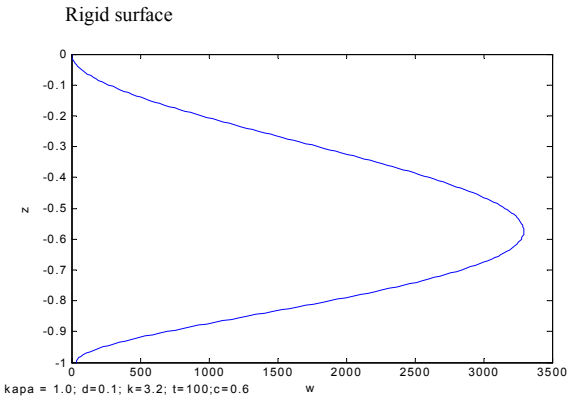

Figure 1: Z vs. w;

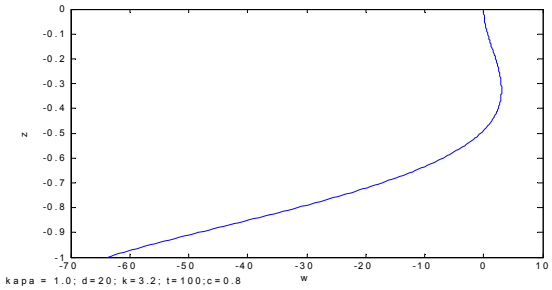

Figure 2: Z vs. W;

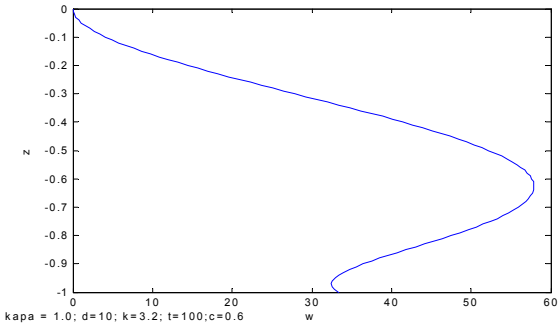

Figure 3: Z vs. w;

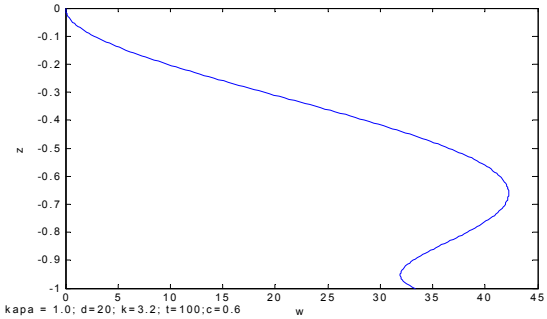

Figure 4: Z vs. W;

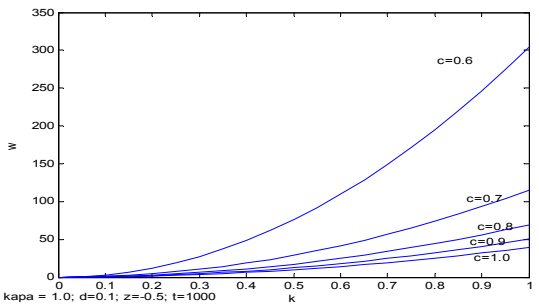

Figure 5a: W vs. K;

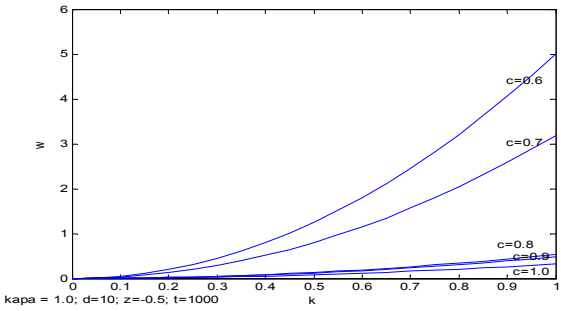

Figure 5b: W vs. k;

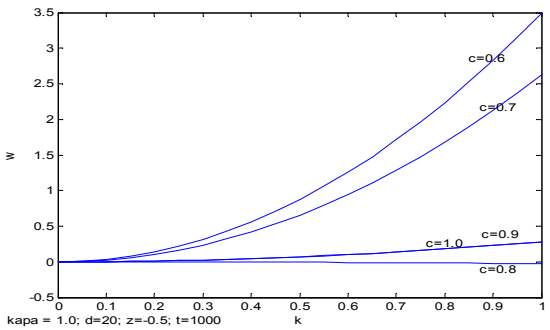

Figure 5c: W vs. k;

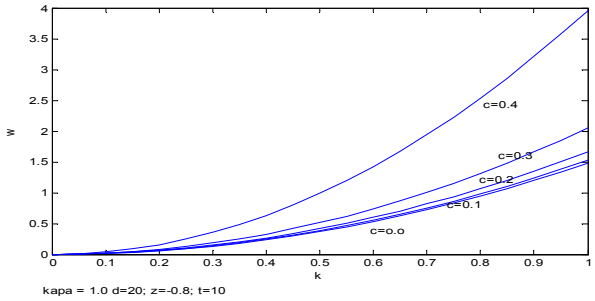

Figure 6a: W vs. k;

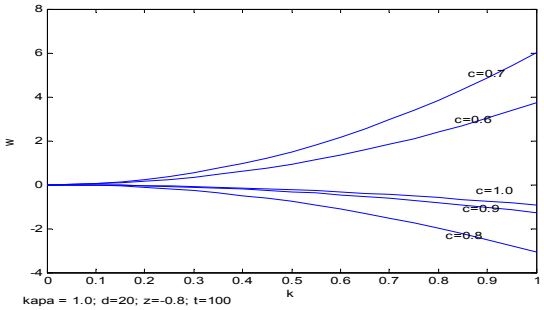

Figure 6b: W vs. K;

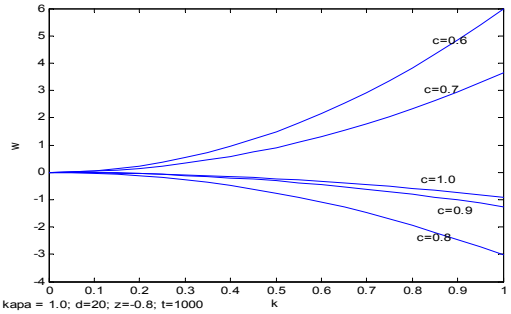

Figure 6c: W vs. K;

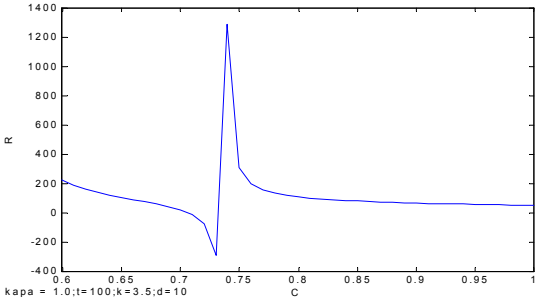

Figure 7: R vs. C;

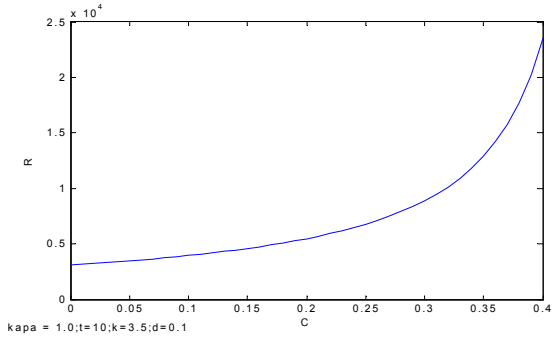

Figure 8: R vs. C;

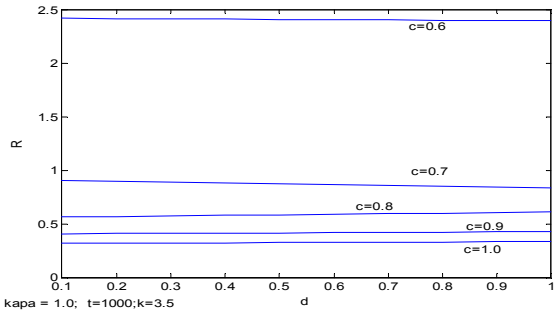

Figure 9: R vs. d;

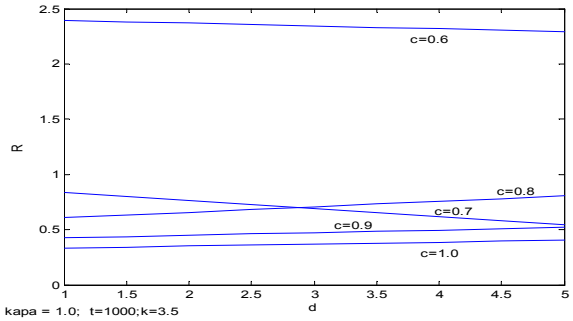

Figure 10: R vs. d;

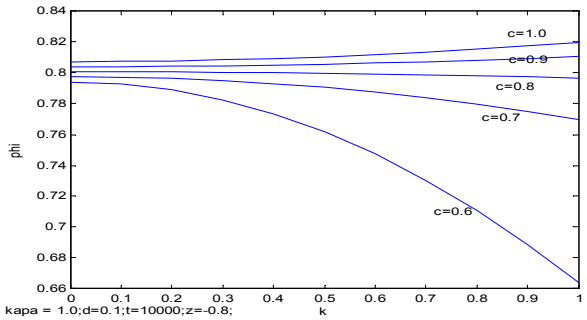

Figure 11: phi

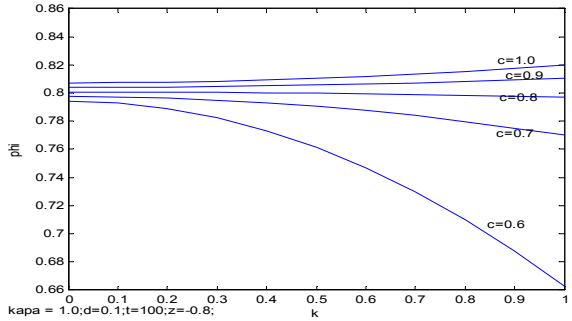

Figure 12: Phi vs. K;

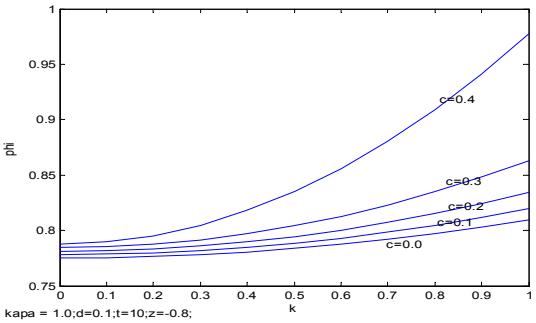

Figure 13: Phi vs. K;

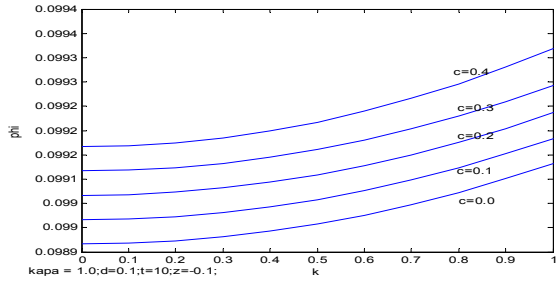

Figure 14: Phi vs. K;

Stress free upper surface

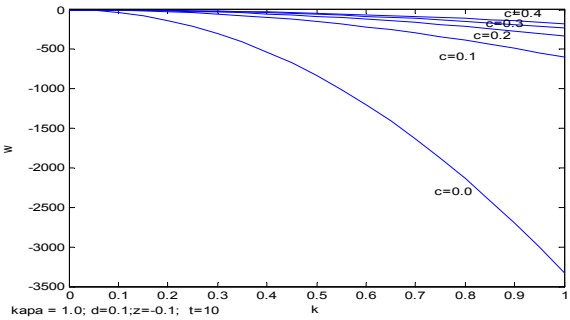

Figure 15 : W vs. K;

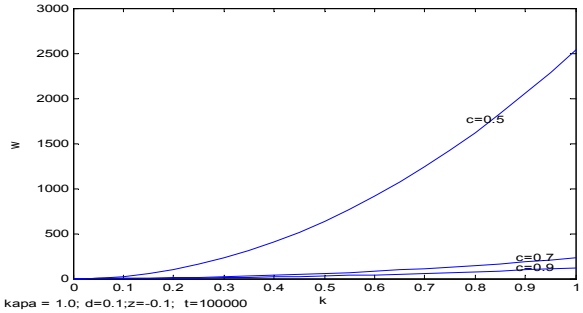

Figure 16: W vs. K;

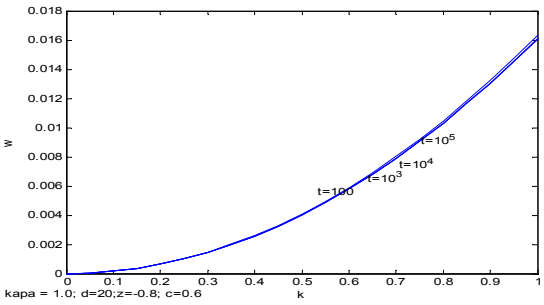

Figure 17: W vs. K;

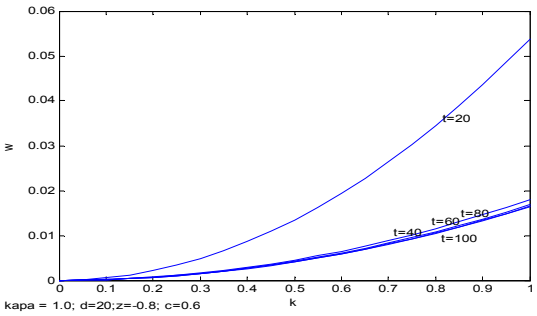

Figure 18: W vs. K;

REFERENCES

Chandrasekhar, S., Hydrodynamics and Hydromantic stability. Oxford University Press. Oxford, 1961

Childress S. Levan dowsky. M and spiegal E A.1975. *J. Fluid Mech.,* 63. 591-613 (referred as CLS).

Hill. N. A and Pedley.T.J . Bio convection, Fluid dynamics research, vol 37.2005.

Mathews. P. C. 1988. A model for the onset of penetrative convection. *J. Fluid Mech., 188*,571-583.

Pedley, T. J. kessler, J O. 1992. Hydrodynamic phenomena in suspensions of gyro tactic micro-organisms. *A. Rev. Fluid Mech.,* 24, 315-358.

Platt.J.r.1961 bio convection patterns in cultures of free swimming algae. Science, 133: 1766-1767.

Rudraiah and Srimani, P.K. 1980. Finite amplitude Cellular convection in a fluid saturated porous layer. Proc.Roy. Soc. London. A. 373, 199.

Srimani .P.K and Sudhakar.H.R.1992. Transitions in heat transfer in a rotating porous layer. Indian journal of pure and applied maths. 23, no6, 1992.

Srimani, P.K. and Anuradha, H.R. 2007. Bio convection patterns in a suspension of gyrotactic microorganisms in a two phased medium .Proc. Int. continuum Mech., 2007.

Srimani, PK. and Padmasini. V. T. 2001. A mathematical model for Bio convection in suspensions of oxytactic bacteria in a two phased system in Proc. SPMV. Computational methods in continuum mechanics in 2001.

Veronis. G..1963. Penetrative convection. Astrophys. J.137.641-663.

Whitehead, J. A. and Chen. M M. 1970.Thermal instability and convection of a thin fluid layer bounded by a stably stratified region. *J.fluid Mech.,* 40, 549-576.

****